PAPER

CrossMark
← click for updates

Combined cytotoxic effect of UV-irradiation and TiO₂ microbeads in normal urothelial cells, low-grade and high-grade urothelial cancer cells

Roghayeh Imani,[a,b] Peter Veranič,[c] Aleš Iglič,[b] Mateja Erdani Kreft,[c] Meysam Pazoki[d] and Samo Hudoklin*[c]

The differentiation of urothelial cells results in normal terminally differentiated cells or by alternative pathways in low-grade or high-grade urothelial carcinomas. Treatments with traditional surgical and chemotherapeutical approaches are still inadequate and expensive, as bladder tumours are generally highly recurrent. In such situations, alternative approaches, using irradiation of the cells and nanoparticles, are promising. The ways in which urothelial cells, at different differentiation levels, respond to UV-irradiation (photolytic treatment) or to the combination of UV-irradiation and nanoparticles (photocatalytic treatment), are unknown. Here we tested cytotoxicity of UV-irradiation on (i) normal porcine urothelial cells (NPU), (ii) human low-grade urothelial cancer cells (RT4), and (iii) human high-grade urothelial cancer cells (T24). The results have shown that 1 minute of UV-irradiation is enough to kill 90% of the cells in NPU and RT4 cultures, as determined by the live/dead viability assay. On the other hand, the majority of T24 cells survived 1 minute of UV-irradiation. Moreover, even a prolonged UV-irradiation for 30 minutes killed <50% of T24 cells. When T24 cells were pre-supplemented with mesoporous TiO₂ microbeads and then UV-irradiated, the viability of these high-grade urothelial cancer cells was reduced to <10%, which points to the highly efficient cytotoxic effects of TiO₂ photocatalysis. Using electron microscopy, we confirmed that the mesoporous TiO₂ microbeads were internalized into T24 cells, and that the cell's ultrastructure was heavily compromised after UV-irradiation. In conclusion, our results show major differences in the sensitivity to UV-irradiation among the urothelial cells with respect to cell differentiation. To achieve an increased cytotoxicity of urothelial cancer cells, the photocatalytic approach is recommended.

Introduction

The urothelium is a unique three layered epithelium that covers most of the mammalian urinary tract, including the urinary bladder, and is responsible for maintaining the tightest permeability barrier in the human body, the so-called blood–urine permeability barrier.[1–4] In a normal urothelium, the formation and maintenance of the blood–urine barrier depends on the processes of urothelial differentiation. These include: (i) the characteristic structure of the cell's apical plasma membrane, (ii) the low-level of molecule internaliz-ation into cells, and (iii) the highly resistant tight junctions.[5–10] Superficial urothelial cells synthesize urothelium-specific transmembrane proteins, uroplakins (UPs),[11,12] which are glycosylated in the Golgi apparatus, arranged into 16 nm particles and are organized into detergent resistant 2D crystals, called urothelial plaques.[13–17] During cell differentiation and during the filling of the bladder with urine, urothelial plaques are being transported to the apical plasma membrane with the fusiform vesicles.[18,19] 70–90% of the apical plasma membrane is therefore covered with the plaques, which significantly contributes to the transcellular barrier of the urothelial cells and gives their luminal membrane a characteristic scalloped appearance.[20]

Moreover, internalization studies have shown that endocytotic activity is 43% to 86% lower in differentiated superficial urothelial cells in comparison with the partially differentiated urothelial cells, and 5 to 15-times lower than in polarized MDCK cells, which contain no urothelial plaques.[21] Therefore, for the intact blood–urine permeability barrier the normal urothelial differentiation with the urothelial plaque formation and a reduced internalization rate is necessary.[22–24]

[a]*Laboratory of Clinical Biophysics, Faculty of Health Sciences, University of Ljubljana, Zdravstvena 5, Ljubljana, Slovenia*
[b]*Laboratory of Biophysics, Faculty of Electrical Engineering, University of Ljubljana, Tržaška 25, Ljubljana, Slovenia*
[c]*Institute of Cell Biology, Faculty of Medicine, University of Ljubljana, Vrazov trg 2, Ljubljana, Slovenia. E-mail: samo.hudoklin@mf.uni-lj.si*
[d]*Department of Chemistry, Ångström Laboratory, Physical Chemistry, University of Uppsala, Box 523, SE 75120 Uppsala, Sweden*

This journal is © The Royal Society of Chemistry and Owner Societies 2015

Photochem. Photobiol. Sci., 2015, **14**, 583–590 | 583

On the other hand, urothelial differentiation can also take alternative pathways, which result in the urinary bladder cancer with an inverse relation of the differentiation level to the cancer cell grade.[3,25] The urothelial cancer is the 4th most common type of cancer in men, with 430 000 new diagnoses worldwide every year.[26,27] Current approaches to the treatment of the most common urothelial cancer in humans include the transurethral papilloma resection and the local application of chemotherapy or immunotherapy.[28,29] The high rate of recurrence makes these treatments rather inadequate and the lifetime treatment and monitoring costs of patients with urothelial carcinomas are the highest among of all cancers.[26] To this end, alternative or supplemental approaches to treatment are being tested, including photocatalytic treatments. The rationale behind the photocatalytic treatment of bladder cancer consists of 2 steps: (i) urothelial cancer cells are at a lower level of differentiation and they can therefore internalize more nanoparticles than normal, highly differentiated urothelial cells, and (ii) the irradiation of cells with sufficient energy (e.g. UV-irradiation) would cause a photocatalytic generation of reactive oxidative species (ROS) in the cells with internalized nanoparticles, which would in turn cause sufficient cytotoxic effects (e.g. lipid, protein and DNA lesions) to lethally damage cancer cells.

Recently, titanium dioxide (TiO_2) has emerged as an excellent biocompatible photocatalyst material.[19,30,31] In particular, TiO_2 has been useful as a catalyst for the photodegradation of organic compounds and the deactivation of microorganisms by photogenerated ROS.[32,33] It has been reported that various ROS, such as superoxide ($O_2^{\bullet-}$), singlet oxygen ($^1O_2$), the hydroxyl radical ($^{\bullet}OH$), the hydroperoxyl radical ($HO_2^{\bullet}$), and hydrogen peroxide (H_2O_2), are generated on the TiO_2 surface and react with organic or inorganic compounds in the gas and liquid phases.[34] Studies have shown that the geometry of nanoparticles may have a significant effect on the photoelectrolysis activity.[34] In addition, the photocatalytic activity of TiO_2 crystals is heavily dependent on the surface structure, including surface atomic arrangement and coordination, especially when the particle size is reduced to the nanometer scale, leading to a large effective surface area.[35,36]

UV-irradiation is well known for its cytotoxic effects, among which DNA lesions and their consequences have been studied in great detail.[37] In general, DNA molecules exhibit strong UV absorption in the wavelength range of ~220–300 nm, with the maximum peak at 260 nm and act as the major cellular chromophores for the UV-C spectrum of irradiation.[38] The direct absorption of UV-irradiation induces the formation of cyclobutane pyrimidine (CPD) dimers, (6-4) pyrimidine-pyrimidone photoproducts and their Dewar isomers,[39] which if unrepaired would block the transcription of DNA genes to RNA and would eventually lead to the cell death or initiate photocarcinogenesis.[40,41]

To the best of our knowledge, the cytotoxic effects of UV-irradiation on differently differentiated urothelial cells have not yet been studied. In this paper, we studied the sensitivity of three differently differentiated cultures of urothelial cells to UV-irradiation. To increase the photocatalytic damage and the selectivity of treatment to high-grade urothelial cancer cells, the cells were supplemented with mesoporous TiO_2 microbeads before exposing them to UV-irradiation.
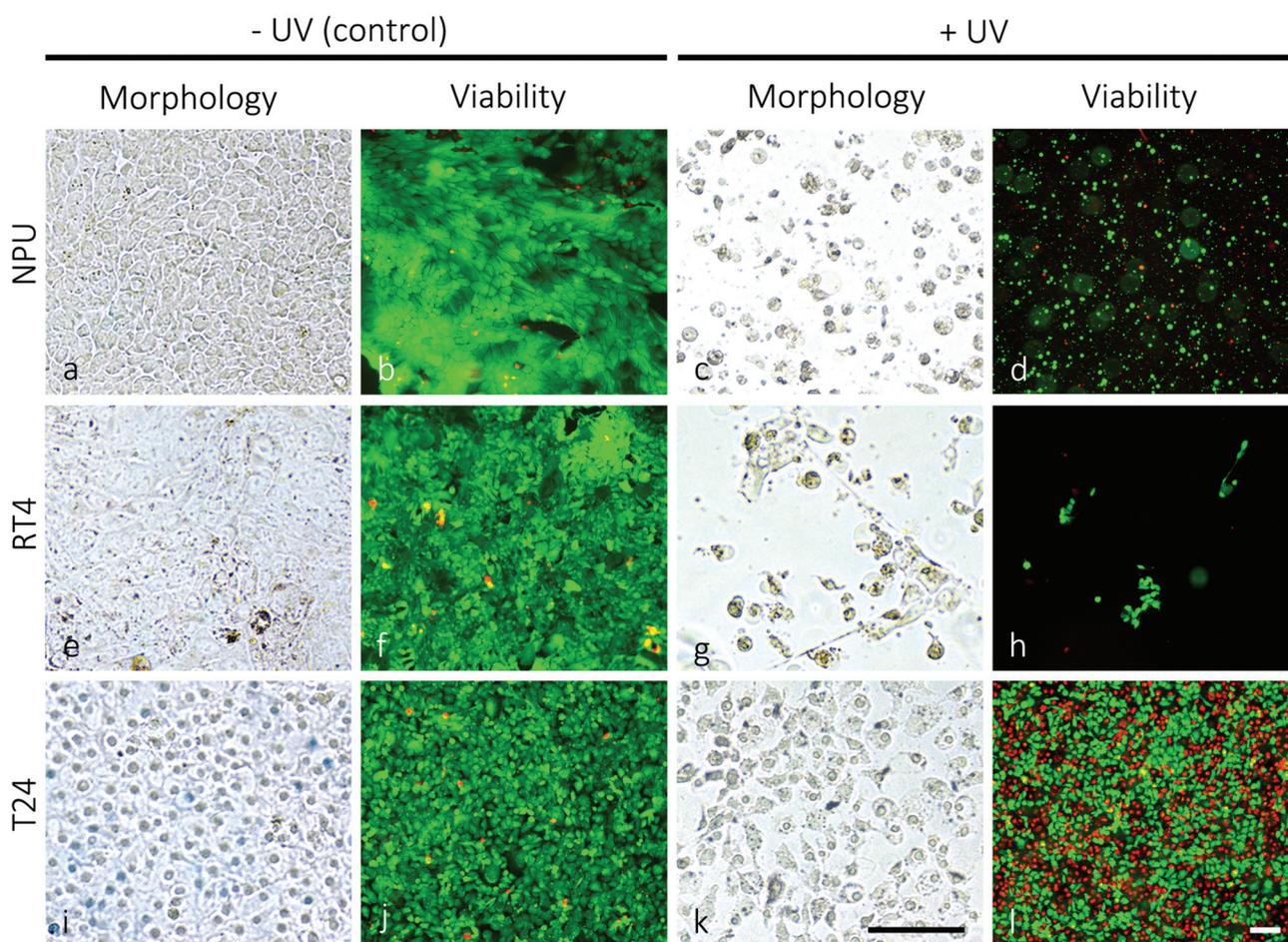
Results and discussion

The UV-spectrum is divided into three regions UV-A (315–400 nm), UV-B (280–315) nm and UV-C (100–280 nm). For phototherapies used in clinics for the treatment of pathologies, such as psoriasis, vitiligo, atopic dermatitis or mycosis fungoides, relatively non-harmful UV-A and UV-B spectra are generally used.[42,43] On the other hand, for the purpose of efficiently killing urothelial cancer cells, UV-C irradiation was chosen, which has the highest energy content among UV-spectra and causes the most damaging effects to the cells.[44]

Cell treatment showed that normal porcine urothelial cells (NPU) and human low-grade non-invasive cancer RT4 cells are significantly more prone to UV-irradiation damage than human high-grade and invasive urothelial cancer T24 cells. Twenty-four hours after 1 minute of UV-irradiation, the morphological and ultrastructural appearance of NPU and RT4 cell cultures changed from confluent with polygonal cells (Fig. 1a and e) to sporadic with frequently rounded cells (Fig. 1c and g). Many cells were detached and floated in the growth medium. The live/dead viability assay indicated a high level of cytotoxicity of UV-irradiation for NPU and RT4 cells: in the control cultures the cells were >95% live (labelled green; Fig. 1b and f), while in the UV-irradiated cultures there remained <10% live cells (Fig. 1d and h). On the other hand, the morphological appearance of irradiated T24 cells remained unchanged 24 hours after 1 minute of UV-irradiation (figures not shown). The live/dead viability assay showed that T24 cells were still viable after such a treatment. Moreover, even after prolonged UV-irradiation (30 minutes), the morphology of the T24 cultures remained mainly unchanged (Fig. 1i and k), with the majority of cells being viable (Fig. 1j and l). Neither NPU nor RT4 cells survived 30 minutes of UV-irradiation.

Our results showed that even relatively high doses of very photolytic UV-C irradiation did not eliminate all high-grade urothelial cancer cells. It is not likely that the DNA of high-grade urothelial cancer cells is better protected or less susceptible to UV-C irradiation damage in comparison to the DNA of more differentiated cells.[45] In some cell types, very proficient DNA repair systems were found to cope with various kinds of DNA damage: mismatch repair, base excision repair, direct damage reversal, double strand break repair and nucleotide excision repair.[46,47] The better survival of less differentiated T24 cells is in accordance with the studies that show that the DNA repair system is differentiation dependent.[48] In general, the repair system is attenuated with the progression of cell differentiation: in rat neurons, chicken striated muscles, human macrophages, mouse keratinocytes and others.[48,49] We suggest that urothelial high-grade cancer cells, which are at a lower differentiation stage than the RT4 and NPU cells, are

584 | *Photochem. Photobiol. Sci.*, 2015, **14**, 583–590

This journal is © The Royal Society of Chemistry and Owner Societies 2015

Fig. 1 Morphology and viability of normal porcine urothelial cells (NPU), and cancer RT4 and T24 cells in control and UV-irradiated cultures. Note the changed morphology and the reduced number of NPU (c) and RT4 cells (g) 24 hours after 1 minute of UV-irradiation in comparison to their non-irradiated controls (a, e). The number of NPU and RT4 cells labeled green (live cells) has significantly decreased after the UV-irradiation (d, h *versus* b, f). The cells labelled red (dead cells) were detached from the growth medium and are therefore not seen on the panels (d, h). On the other hand, the high fraction of T24 cells retained their morphology and survived 24 hours after 30 minutes of UV-irradiation (k, l *versus* i, j). Legend: green − live cells, red − dead cells. Bars: 100 μm.

also more resistant to structural lesions and apoptosis,[50] which makes for the difference in the cells' survival rate.

To test the cytotoxic potential of mesoporous TiO_2 microbead photocatalysis and to increase the selectivity in damaging the predominantly less differentiated urothelial cancer cells with an elevated level of endocytotic activity, the growth medium of T24 cells was supplemented with mesoporous TiO_2 microbeads. The mesoporous TiO_2 microbeads were prepared by the solvothermal method. These microbeads are monodispersed TiO_2 with a diameter of 600 ± 100 nm (Fig. 2). The microbeads have rough surfaces made of ∼15 nm sized TiO_2 nanocrystals organized in such a way that they form pores into the internal structure of the microbeads. High surface area, light harvesting and scattering efficiency together with their high crystallinity make them very promising for killing the cancer cells (data under publication elsewhere).

Crystallinity and low trap density of the microbeads, which allows the fast diffusion of electrons, facilitate electron donating properties (*i.e.* higher reactive oxidative species generation)
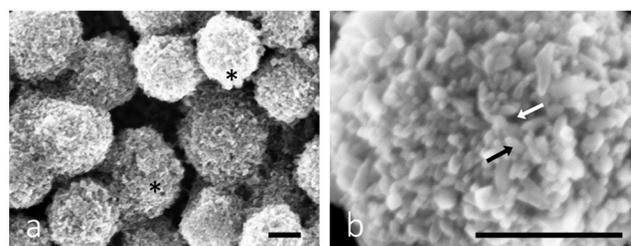
Fig. 2 Scanning electron microscopy image of mesoporous TiO_2 microbeads in (a) low and (b) high magnification. Legend: asterisks − microbeads, black arrow − individual TiO_2 particle, white arrow − pores in the surface structure of the microbead. Bars: 250 nm.

and impede the electron–hole recombination processes, are possible reasons for the high efficiency of the here used TiO_2 microbeads compared to commercial nanoparticles.[51]

Such mesoporous TiO_2 microbeads were left to be internalized by T24 urothelial cancer cells. The leftovers of the

microbeads were removed from the growth medium, and subsequently the cultures were UV-irradiated for 30 minutes. The live/dead viability assay revealed that 24 hours after irradiation the viability of T24 cells pre-supplemented with mesoporous TiO_2 microbeads was significantly reduced in comparison with T24 cells that were UV-irradiated, but contained no mesoporous TiO_2 microbeads (Fig. 3a and d). The mesoporous TiO_2 microbeads alone proved to be non-toxic for the cells (Fig. 3b). When the T24 cultures were UV-irradiated, 58% of the cells were labelled green (Fig. 3c), and were thus live, while in the UV-irradiated cultures pretreated with mesoporous TiO_2 microbeads there were <10% of the green labelled cells (Fig. 3d). Scanning and transmission electron microscopy was used to localize the mesoporous TiO_2 microbeads in the cell culture and determine their photocatalytic effects on the cell's ultrastructure (Fig. 3e–l). Mesoporous TiO_2 microbeads were located at the apical side of the plasma membranes and intracellularly, in the membrane compartments (Fig. 3h, j and l).

Occasionally, mesoporous TiO_2 microbeads were located in T24 cells in the invaginations characteristic of phagocytosis (Fig. 3l). The ultrastructure of the examined cells pre-treated with TiO_2 microbeads and UV-irradiated (Fig. 3l) was significantly changed in comparison to control cells and to the TiO_2 microbead pre-treated or UV-irradiated only cells (Fig. 3i–k). In the UV-irradiated cells loaded with mesoporous TiO_2 microbeads, the plasma membrane was discontinuous, clearly showing holes (Fig. 3h). Their cytoplasm lost its fine, homogeneous appearance and looked washed out (Fig. 3l). The cell's intracellular membrane compartments were distended, with ruptured internal membrane structures, which is a known characteristic of the necrotic cells. The emphasized necrotic cell death is most likely a consequence of the photocatalytic effects of mesoporous TiO_2 microbeads pre-supplemented to the cells. The photocatalysis of TiO_2 generally involves four processes: (i) the generation of electrons and holes by photoexcitation; (ii) the migration of the photo-
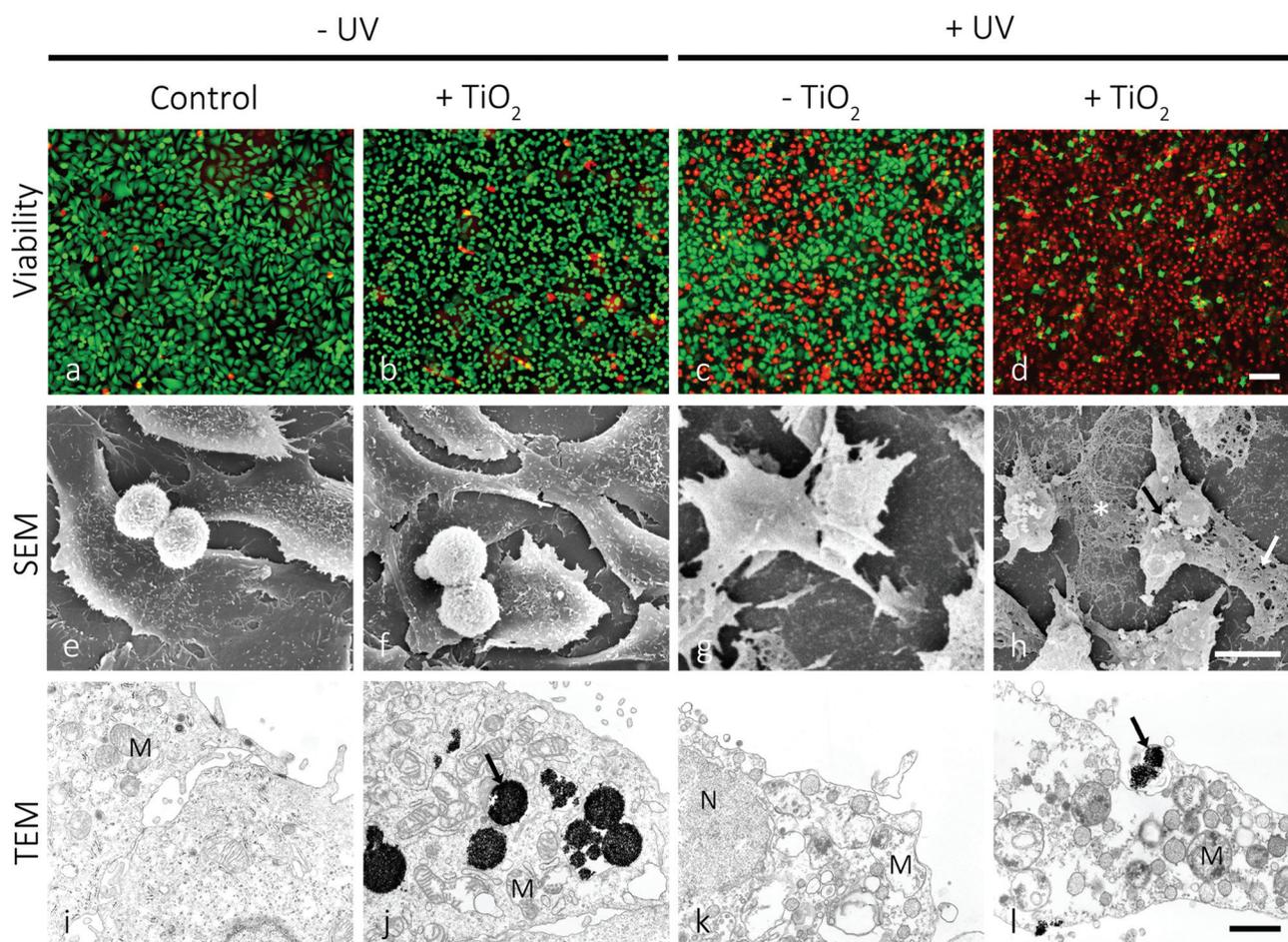

Fig. 3 Viability, scanning- and transmission electron microscopy of high-grade urothelial cancer T24 cells 24 hours after the treatment. The first column shows control cells, the second column the cells pre-treated with mesoporous TiO_2 microbeads, but not exposed to UV-irradiation, the third column shows the cells exposed to UV-irradiation for 30 minutes, and the fourth column shows the cells pre-treated with mesoporous TiO_2 microbeads and UV-irradiated for 30 minutes. Note that in the last column there is a significantly increased number of cells labelled red (dead cells; d), and that perforations (white arrow; h) can be seen in the apical plasma membrane of the cells and TiO_2 microbeads (black arrow; l), associated with the damaged cell's ultrastructure. Legend: green – live cells, red – dead cells, asterisk – remains of the cell, black arrows – TiO_2 microbeads, white arrow – perforation in the plasma membrane, M – mitochondria. Bars: a–d – 100 µm, e–h – 10 µm, i–l – 1 µm.

586 | *Photochem. Photobiol. Sci.*, 2015, **14**, 583–590

This journal is © The Royal Society of Chemistry and Owner Societies 2015

generated charge carriers to the surface of TiO_2 microbeads; (iii) the subsequent reduction/oxidization of the adsorbed reactants directly by electrons/holes or indirectly by ROS; and (iv) the recombination of the photogenerated electron–hole pairs. The efficient photocatalytic material is expected to promote processes (i), (ii), and (iii) and to suppress process (iv).[36]

The mesoporous microbeads used here consist of a bundle of ~15 nm sized TiO_2 particles, which form sub-micron porous spheres with the superior light-harvesting properties in comparison to the photocatalytic material made of small individual particles. Moreover, mesoporous TiO_2 microbeads were not only shown to exhibit strong UV-light scattering properties, but the interface of small TiO_2 crystallites in the microbeads can also lead to a faster diffusion of electrons, which is beneficial for photocatalysis and may also affect the electron–hole recombination.[52,53] Therefore, the selective internalization of TiO_2 microbeads used here facilitates the production of ROS after UV-irradiation, and can be recommended for efficient and selective treatment of cancer cells.[54]

The synergistic effect of the here tested combined treatment with TiO_2 and UV-irradiation suits well to the clinical demands and recent experimental findings in the treatment of bladder cancer. In clinical praxis the main problem in treating bladder cancer is not how to eliminate the main population of cancer cells, but in the accessibility of drugs to the remaining cancer cells, as they represent seeds for the new urothelial tumours.[55] After the conventional treatment these remaining cancer cells are supposed to spread within the normal urothelium where they are protected from chemotherapeutic drugs by the tight blood–urine barrier of normal urothelial cells (Fig. 4a). Such persisting cancer cells are supposed to be mainly responsible for the relapse of bladder tumours.[56] Therefore, in order to treat hidden cancer cells, it is necessary to remove the superficial layer of differentiated urothelial cells (umbrella cells; Fig. 4b) in the first step. UV-C irradiation used here was proved to be successful in the removal of normal superficial cells, while the cell irradiated with longer wavelengths (e.g. UV-A) failed to remove these cells (unpublished data). In the second step, the highly efficient light harvesting photocatalytic material introduced into urinary bladder lumen (i.e. TiO_2 microbeads) should be internalized into the cancer cells (Fig. 4c). We have recently proven that less differentiated have a highly increased potential of endocytosis in comparison to normal urothelial cells (ref. 7 and unpublished results) giving a strong emphasis on the selectivity of such a treatment. Next, the enhanced phototoxicity of UV-irradiation in cells that endocytosed TiO_2 microbeads speaks well in favour of the selective treatment of exposed cancer cells after the removal of umbrella cell shield by UV-C irradiation (Fig. 4d and e). Since the energy for generating the photocatalytic effects of TiO_2 microbeads can be lower than the one needed for the removal of the umbrella cells, one might reduce the intensity of UV-C irradiation to harm only the cancer cells or use UV-A irradiation in this step. That would selectively kill cancer cells containing microbeads, but preserve normal cells in the urothelium. Finally, the regeneration and differentiation of the
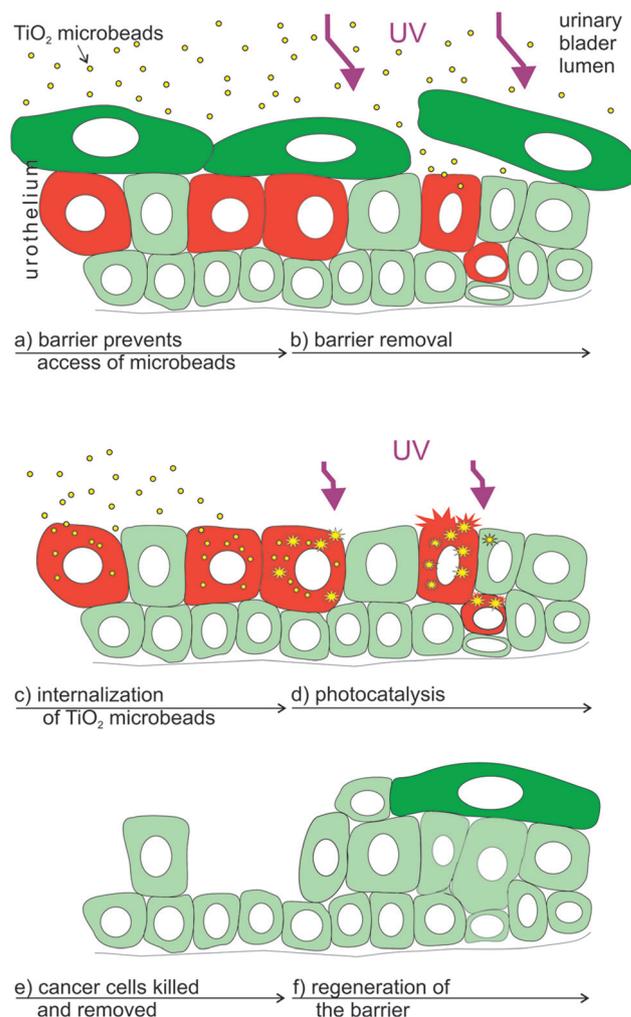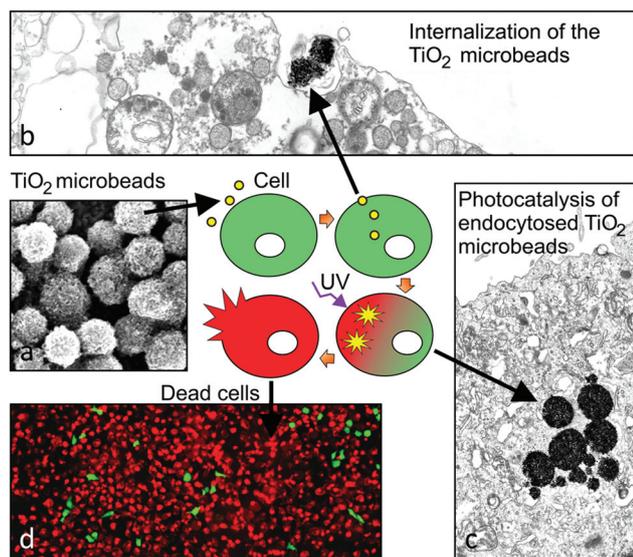

Fig. 4 Scheme of the proposed supplemental treatment of the *in vivo* urinary bladder cancer by a combination of UV-irradiation and TiO_2 microbeads. Legend: red – cancer cells, green – normal urothelial cells (dark green depicts differentiated urothelial cells), purple – UV-irradiation (smaller arrows in d depict irradiation with reduced intensity or one with less-energy in comparison to a).

remaining normal urothelial cells restores the urothelium and its blood–urine barrier function (Fig. 4f). Exceedingly rapid regeneration of the urothelial tissue, recovering within less than an hour, also prevents unfavourable effects of the barrier removal and the potential toxic effect on regenerating normal cells, caused by UV-C irradiation.[57]

Conclusions

Our results clearly show the increase in the toxicity to high-grade urothelial cancer cells when the UV-irradiation of cells was combined with TiO_2 microbead application (Fig. 5). These results could provide useful information for further studies in searching for selective anticancer treatment of urothelial and other epithelial tumours.

This journal is © The Royal Society of Chemistry and Owner Societies 2015

Photochem. Photobiol. Sci., 2015, **14**, 583–590 | 587

Fig. 5 Schematic presentation of the mechanism for the cytotoxic potential of photocatalytic TiO_2 microbeads in high grade urothelial cancer cells. (a) Mesoporous TiO_2 microbeads are supplemented into the lumen of urinary bladder, where they interact with (b) and are endocytosed (c) preferably by cancer cells, which are at the lower stage of differentiation. (d) The UV-irradiation of microbeads triggers the photocatalytic production of reactive oxidative species, which highly increases the efficiency of killing cancer cells.

Experimental

Cell cultures

Three types of urinary bladder epithelial cells were used for the experiments: normal porcine urothelial cells (NPU; cells isolated from a healthy pig and further prepared and differentiated as described previously),[58] the RT4 cell line (human low-grade and noninvasive urothelial carcinoma cells), and the T24 cell line (human high-grade and invasive urothelial carcinoma cells). Each type of cells was seeded on glass coverslips within Petri dishes and cultured to >85% confluence in the UroM or advanced-DMEM-F12 medium as described previously.[6,59] Petri dishes were then divided into 2 groups: (1) the control group and (2) the experimental group (+UV). Normal porcine urothelial cells, RT4 and T24 cells of the experimental group were irradiated for 1 or 30 minutes with the UV-C light (Sylvania Ultra Violet G15W; 15 W cm^{-2}); the irradiation of the cells in the control group was omitted. In the next step, cells were grown for additional 24 hours in the CO_2-incubator at 37 °C under a humidified atmosphere of 5% CO_2 (v/v), and were subsequently sampled for morphology, live/dead viability assay, and ultrastructural analysis.

Mesoporous TiO_2 microbeads synthesis and characterization

Mesoporous TiO_2 microbeads were synthesized by the solvothermal method according to our previous report.[51] The mesoporous TiO_2 microbead particle morphology was examined with a S4700 scanning electron microscope (Hitachi).

Morphological characterization of the cells

The samples of the control and experimental cell cultures were examined unprocessed. The samples were taken from the CO_2-incubator and were immediately inspected with the T300 phase-contrast light microscope (Nikon).

Live/dead viability assay

To evaluate the cytotoxic effects of the mesoporous TiO_2 microbeads and UV-light irradiation, a Live/Dead Viability Kit (Invitrogen, Life Technologies) was used. Cells attached to the coverslips were processed according to the manufacturer's protocol, and visualized and photographed 25 minutes after adding the kit with a T300 fluorescence-light microscope (Nikon). The green signal characterized the live cells and the red signal characterized the dead cells. For each cell group, four coverslips and five fields on each coverslip were examined.

To evaluate the cytotoxic effect of the mesoporous TiO_2 microbeads in combination with UV-irradiation, T24 cells were incubated for 2 hours in the cell growth medium, supplemented with 50 μg ml^{-1} of mesoporous TiO_2 microbeads. Afterwards the medium was changed for a fresh one without the TiO_2 microbeads, and the cell cultures were irradiated for 30 minutes as above. After 24 hours, the cultures were sampled for the morphological study, the live/dead viability assay, transmission electron microscopy (TEM) and scanning electron microscopy (SEM) analysis.

Ultrastructural analysis

Samples were fixed with 4% formaldehyde and 2% glutaraldehyde in 0.1 M cacodylate buffer and subsequently processed for TEM and SEM. For TEM, samples were embedded in Epon, sectioned, counterstained and examined with a CM100 TEM (Philips) operating at 80 kV. For SEM, the samples were dehydrated, dried, sputter-coated and examined with a JSM840A SEM (Jeol) at 15 kV.

Acknowledgements

Notes and references

1 M. E. Kreft, S. Hudoklin, K. Jezernik and R. Romih, *Protoplasma*, 2010, **246**, 3–14.
2 F. X. Liang, M. C. Bosland, H. Huang, R. Romih, S. Baptiste, F. M. Deng, X. R. Wu, E. Shapiro and T. T. Sun, *J. Cell Biol.*, 2005, **171**, 835–844.

3 X. R. Wu, X. P. Kong, A. Pellicer, G. Kreibich and T. T. Sun, *Kidney Int.*, 2009, **75**, 1153–1165.

4 H. O. Negrete, J. P. Lavelle, J. Berg, S. A. Lewis and M. L. Zeidel, *Am. J. Physiol.*, 1996, **271**, F886–F894.

5 S. A. Lewis and J. M. Diamond, *J. Membr. Biol.*, 1976, **28**, 1–40.

6 T. Visnjar and M. E. Kreft, *In Vitro Cell. Dev. Biol.: Anim*, 2013, **49**, 196–204.

7 M. E. Kreft, K. Jezernik, M. Kreft and R. Romih, *Ann. N. Y. Acad. Sci.*, 2009, **1152**, 18–29.

8 R. Romih, P. Korosec, W. de Mello Jr. and K. Jezernik, *Cell Tissue Res.*, 2005, **320**, 259–268.

9 R. Romih, P. Veranic and K. Jezernik, *Appl. Immunohistochem. Mol. Morphol.*, 2002, **10**, 339–343.

10 P. Veranic, R. Romih and K. Jezernik, *Eur. J. Cell Biol.*, 2004, **83**, 27–34.

11 X. R. Wu, M. Manabe, J. Yu and T. T. Sun, *J. Biol. Chem.*, 1990, **265**, 19170–19179.

12 J. Yu, M. Manabe, X. R. Wu, C. Xu, B. Surya and T. T. Sun, *J. Cell Biol.*, 1990, **111**, 1207–1216.

13 B. Kachar, F. Liang, U. Lins, M. Ding, X. R. Wu, D. Stoffler, U. Aebi and T. T. Sun, *J. Mol. Biol.*, 1999, **285**, 595–608.

14 G. Min, H. Wang, T. T. Sun and X. P. Kong, *J. Cell Biol.*, 2006, **173**, 975–983.

15 F. X. Liang, I. Riedel, F. M. Deng, G. Zhou, C. Xu, X. R. Wu, X. P. Kong, R. Moll and T. T. Sun, *Biochem. J.*, 2001, **355**, 13–18.

16 S. Hudoklin, D. Zupancic and R. Romih, *Cell Tissue Res.*, 2009, **336**, 453–463.

17 C. C. Hu, T. Bachmann, G. Zhou, F. X. Liang, J. Ghiso, G. Kreibich and T. T. Sun, *Biochem. J.*, 2008, **414**, 195–203.

18 S. Hudoklin, K. Jezernik, J. Neumuller, M. Pavelka and R. Romih, *PLoS One*, 2012, **7**, e32935.

19 P. Kocbek, K. Teskac, M. E. Kreft and J. Kristl, *Small*, 2010, **6**, 1908–1917.

20 S. A. Lewis, *Am. J. Physiol. Renal Physiol.*, 2000, **278**, F867–F874.

21 M. E. Kreft, R. Romih, M. Kreft and K. Jezernik, *Differentiation*, 2009, **77**, 48–59.

22 P. Hu, F. M. Deng, F. X. Liang, C. M. Hu, A. B. Auerbach, E. Shapiro, X. R. Wu, B. Kachar and T. T. Sun, *J. Cell Biol.*, 2000, **151**, 961–972.

23 P. Hu, S. Meyers, F. X. Liang, F. M. Deng, B. Kachar, M. L. Zeidel and T. T. Sun, *Am. J. Physiol. Renal Physiol.*, 2002, **283**, F1200–F1207.

24 X. T. Kong, F. M. Deng, P. Hu, F. X. Liang, G. Zhou, A. B. Auerbach, N. Genieser, P. K. Nelson, E. S. Robbins, E. Shapiro, B. Kachar and T. T. Sun, *J. Cell Biol.*, 2004, **167**, 1195–1204.

25 P. Khandelwal, S. N. Abraham and G. Apodaca, *Am. J. Physiol. Renal Physiol.*, 2009, **297**, F1477–F1501.

26 K. D. Sievert, B. Amend, U. Nagele, D. Schilling, J. Bedke, M. Horstmann, J. Hennenlotter, S. Kruck and A. Stenzl, *World J. Urol.*, 2009, **27**, 295–300.

27 L. W. Fei Ye, M. Castillo-Martin, R. McBride, M. D. Galsky, J. Zhu, P. Boffetta, D. Y. Zhang and C. C.-C. Zhang, *Am. J. Clin. Exp. Urol.*, 2014, **2**, 1–14.

28 J. Bhatt, N. Cowan, A. Protheroe and J. Crew, *Expert Rev. Anticancer Ther.*, 2012, **12**, 929–939.

29 R. K. Lee, H. Abol-Enein, W. Artibani, B. Bochner, G. Dalbagni, S. Daneshmand, Y. Fradet, R. E. Hautmann, C. T. Lee, S. P. Lerner, A. Pycha, K. D. Sievert, A. Stenzl, G. Thalmann and S. F. Shariat, *BJU Int.*, 2014, **113**, 11–23.

30 M. Li, G. Huang, Y. Qiao, J. Wang, Z. Liu, X. Liu and Y. Mei, *Nanotechnology*, 2013, **24**, 305706.

31 A. L. Linsebigler, G. Lu and J. T. Yates, *Chem. Rev.*, 1995, **95**, 735–758.

32 G. Gogniat and S. Dukan, *Appl. Environ. Microbiol.*, 2007, **73**, 7740–7743.

33 Y. Guo, C. Cheng, J. Wang, Z. Wang, X. Jin, K. Li, P. Kang and J. Gao, *J. Hazard Mater.*, 2011, **192**, 786–793.

34 M. R. Hoffmann, S. T. Martin, W. Choi and D. W. Bahnemann, *Chem. Rev.*, 1995, **95**, 69–96.

35 G. K. Mor, K. Shankar, M. Paulose, O. K. Varghese and C. A. Grimes, *Nano Lett.*, 2005, **6**, 215–218.

36 N. Wu, J. Wang, N. Tafen de, H. Wang, J. G. Zheng, J. P. Lewis, X. Liu, S. S. Leonard and A. Manivannan, *J. Am. Chem. Soc.*, 2010, **132**, 6679–6685.

37 M. Ljungman and F. Zhang, *Oncogene*, 1996, **13**, 823–831.

38 J. S. Taylor, *Acc. Chem. Res.*, 1994, **27**, 76–82.

39 J. L. Ravanat, T. Douki and J. Cadet, *J. Photochem. Photobiol. B*, 2001, **63**, 88–102.

40 R. M. Costa, V. Chigancas, S. Galhardo Rda, H. Carvalho and C. F. Menck, *Biochimie*, 2003, **85**, 1083–1099.

41 L. Proietti De Santis, C. L. Garcia, A. S. Balajee, P. Latini, P. Pichierri, O. Nikaido, M. Stefanini and F. Palitti, *DNA Repair*, 2002, **1**, 209–223.

42 V. Bulat, M. Situm, I. Dediol, I. Ljubicic and L. Bradic, *Coll. Antropol.*, 2011, **35**(Suppl. 2), 147–151.

43 W. Lapolla, B. A. Yentzer, J. Bagel, C. R. Halvorson and S. R. Feldman, *J. Am. Acad. Dermatol.*, 2011, **64**, 936–949.

44 T. D. Cutler and J. J. Zimmerman, *Anim. Health Res. Rev.*, 2011, **12**, 15–23.

45 R. Yin, T. Dai, P. Avci, A. E. Jorge, W. C. de Melo, D. Vecchio, Y. Y. Huang, A. Gupta and M. R. Hamblin, *Curr. Opin. Pharmacol.*, 2013, **13**, 731–762.

46 T. Lindahl and R. D. Wood, *Science*, 1999, **286**, 1897–1905.

47 A. Sancar, L. A. Lindsey-Boltz, K. Unsal-Kacmaz and S. Linn, *Annu. Rev. Biochem.*, 2004, **73**, 39–85.

48 T. Nouspikel, *Neuroscience*, 2007, **145**, 1213–1221.

49 T. Nouspikel and P. C. Hanawalt, *DNA Repair*, 2002, **1**, 59–75.

50 K. Wu, J. Zeng, J. Zhou, J. Fan, Y. Chen, Z. Wang, T. Zhang, X. Wang and D. He, *Urol. Oncol.*, 2013, **31**, 1751–1760.

51 M. Pazoki, N. Taghavinia, A. Hagfeldt and G. Boschloo, *J. Phys. Chem. C*, 2014, **118**(30), 16472–16478.

This journal is © The Royal Society of Chemistry and Owner Societies 2015

Photochem. Photobiol. Sci., 2015, **14**, 583–590 | 589

52 J. A. Wang, R. Limas-Ballesteros, T. López, A. Moreno, R. Gómez, O. Novaro and X. Bokhimi, *J. Phys. Chem. B*, 2001, **105**, 9692–9698.

53 F. Sauvage, D. Chen, P. Comte, F. Huang, L. P. Heiniger, Y. B. Cheng, R. A. Caruso and M. Graetzel, *ACS Nano*, 2010, **4**, 4420–4425.

54 J. Rauch, W. Kolch, S. Laurent and M. Mahmoudi, *Chem. Rev.*, 2013, **113**, 3391–3406.

55 C. Hafner, R. Knuechel, R. Stoehr and A. Hartmann, *Int. J. Cancer*, 2002, **101**, 1–6.

56 M. G. Wientjes, R. A. Badalament, R. C. Wang, F. Hassan and J. L. Au, *Cancer Res.*, 1993, **53**, 3314–3320.

57 P. Veranic, A. Erman, M. Kerec-Kos, M. Bogataj, A. Mrhar and K. Jezernik, *Histochem. Cell Biol.*, 2009, **131**, 129–139.

58 T. Visnjar and M. E. Kreft, *Histochem. Cell Biol.*, 2014, DOI: 10.1007/s00418-014-1265-3.

59 R. Imani, D. Kabaso, M. Erdani Kreft, E. Gongadze, S. Penic, K. Elersic, A. Kos, P. Veranic, R. Zorec and A. Iglic, *Croat. Med. J.*, 2012, **53**, 577–585.